IPPI
Polyolefins Journal, Vol. 13, No. 1 (2026)
DOI: 10.22063/POJ.2026.35801.1378
ORIGINAL PAPER

HDPE composite with barrier property to the evaporative emission of volatile organic compounds to use in fuel tanks

Guilherme Gama Simão and Clodoaldo Saron*

Department of Materials Engineering – Lorena School of Engineering – University of São Paulo - DEMAR-EEL/USP, CEP: 12612-550, Lorena, SP, Brazil

Received: 22 October 2025, Revised: 23 February 2026, Accepted: 16 April 2026

ABSTRACT

High-density polyethylene (HDPE) has been widely used in the automotive industry for the manufacture of fuel tanks due to its properties such as chemical stability, easy processability and low cost. However, the low barrier of the HDPE to evaporative emission of organic fuel is a deficiency. Thus, the fluoridation treatment and combination of the HDPE with layers of polar polymers of high barriers for hydrocarbon permeation are currently the procedures usually employed. In the present study, the aim was to evaluate the changes in the barrier property to fuel permeation of the HDPE through incorporation of organically modified montmorillonite clay Cloisite 30B, generating HDPE/Clay nanocomposites. It was verified that the barrier to the fuel permeation is significantly increased in the HDPE/Clay nanocomposites containing clay at 2 and 3 wt.%, while thermal stability and mechanical properties of the material remain similar to the non-filled polymer. The properties and performance of the HDPE/Clay nanocomposites allow its use in the manufacture of fuel tanks, complying with current regulations for evaporative fuel emissions and proving advantages such as lower production cost and recyclability of the material when compared to the traditional methods using fluoridation treatment or multilayer with polar polymers.
Polyolefins J (2026) 13: 53-62

Keywords: Evaporative permeation; fuel tanks; barrier; nanocomposites; clays.

INTRODUCTION

In recent years, there has been a significant decrease in the levels of gas emissions from vehicles powered by internal combustion engines [1]. The development of more efficient engines and high-performance fuels have been the main factors contributing to these advances [2,3]. On the other hand, another source of atmospheric pollution caused by vehicles is the evaporative emission of volatile organic compounds (VOC) not derived from the combustion process, which the hydrocarbon lost from the fuel tank is the most significant [4].

The fuel tanks of the vehicles initially manufactured with metallic materials were gradually substituted by the polymer high-density polyethylene (HDPE) [5]. The high chemical stability of the HDPE, its low density, which contributes to reducing vehicle weight, its low cost and ease of processing are some of the advantages of the HDPE [6-8].

On the other hand, the VOCs permeation in HDPE is high due to the nonpolar chemical structures and high mobility of the polymer chain in the amorphous portion

*Corresponding Author - E-mail: saron@usp.br

at room temperature [6,9,10]. The world legislation has restricted emissions of VOCs by vehicles [1,3,11-13]. Several directives such as Euro 5 (since 2009) and Euro 6 (since 2014) in Europe and the Partial Zero Emission Vehicles (PZEV) of the Californian Air Resources Board (CARB) in the United States of America have defined the emission levels [14]. In Brazil, the regulations in force from 2021 are the PROCONVE L7 and L8, which establish a limit for evaporative emissions of hydrocarbons in vehicles equipped with spark ignition engines of 0.5 g every 48 hours and 50 $mg.L^{-1}$ of fuel present in the fuel tank [15,16].

In order to improve the barrier properties of the HDPE to fuel permeation (gasoline), some strategies have been used to increase the polarity of the polymer structures, such as fluoridation in HDPE after fuel tank manufacturing or intercalation of the HDPE with layers of polar polymers of high barriers for hydrocarbon permeation such as ethylene-vinyl alcohol copolymer (EVOH) and polyamides (PAs), which are typically applied internally in the fuel tank [17].

In spite of the efficient barrier property, both fluoridation treatment and copolymer layers present disadvantages related to the complexity of the equipment required to manufacturing the fuel tank, higher production cost and difficult recycling of polymer waste generated during manufacturing or post-consumption of polymer waste from the fuel tank after the end of its useful life [12].

According to Berger *et al*. and Lee *et al*., the permeation of molecules with low molar mass across a polymer depends on both chemical and physics factors such as temperature, pressure, polymer crystallinity, crosslinking of the polymer chains and chemical interaction between polymer and permeating molecules. Thus, a higher solubility of the permeating molecules in the polymer as well as fewer physical barriers in polymer structures provide a higher permeation rate [6,9].

In the present study, the aim was to evaluate the changes in HDPE barrier properties against permeation of fuel hydrocarbons and other properties of the polymer with the incorporation of modified montmorillonite nanoclays, generating HDPE/nanoclays nanocomposites for potential application in the manufacture of fuel tanks of vehicles with gasoline engine.

Montmorillonite clays are mineral structures belonging to the smectite group [18]. Layers form these clays with a thickness around 1 nm and an aspect ratio from 100 to 400 nm, presenting a typically hydrophilic character [19]. Thus, the presence of montmorillonite nanoplates in HDPE matrix should decrease the chemical interaction of the polymer with non-polar hydrocarbons that compose the fuel (gasoline), resulting in lower solubility and permeation of the fuel across the fuel tank wall. In the same sense, the geometry of the montmorillonite nanoplates should also cause a physical barrier to fuel diffusion, since the fuel molecules cannot cross these nanoplates. On the other hand, the regular dispersion and distribution of mineral filler into the HDPE matrix is a decisive condition for achieving the effectiveness of the barrier property.

Jain *et al*. developed an important study on the use of montmorillonite clay modified with quaternary ammonium and superficially treated with silane modifier, which verified that the best barrier performance against gasoline is achieved when nanoclay is incorporated at 5 wt.% in HDPE [20]. The control of materials processing is a fundamental condition for dispersion and distribution of nanoclay in HDPE matrix, guaranteeing an efficient barrier to fuel permeation. Ma *et al*. prepared HDPE/montmorillonite nanocomposites by micro-nano torsional laminated extrusion, verifying an improved dispersion and orientation of the filler in nanocomposites, which led to a 42% reduction in oxygen permeability compared to press-molded composites [21].

In the present study, the preparation of HDPE/montmorillonite nanocomposites in an internal mixer under a high shear rate led to an efficient separation of the montmorillonite nanolayers as well as high dispersion and distribution in HDPE matrix. Thus, the best barrier to gasoline permeation was achieved with montmorillonite incorporated into the HDPE at 2 wt.% as well as insignificant changes in the thermal and mechanical performance of the polymer.

EXPERIMENTAL

Materials

Virgin high-density polyethylene (HDPE) grade HS4506-Braskem in the form of pellets was donated by IPA Automotive Products Industry RGS Ltda - Brazil, while the organically modified montmorillonite clay Cloisite 30B (Clay) in the powder form with particle size smaller than 13 μm was supplied by Southern Clay Products Inc. Fuel (gasoline) was of commercial grade, which is composed by a mixture of hydrocarbons at 73 V% and anhydrous ethanol at 27 V%. All permeation tests were carried out with the

same fuel sample.

Nanocomposites preparation

Compositions of HDPE/Clay were initially prepared with clay content at 0, 1, 2, 3, 4 and 5 wt.% and packaged in plastic bags. Then, the compositions were processed in a single screw extruder Imacon with a temperature profile of 150, 170, 200 and 200 ºC from hopper to die exit and screw rotation at 50 rpm to generate the respective nanocomposites. A specific screw configuration consisting of Maddock and pineapple mixer geometric elements, was used to improve both the dispersion and distribution of the clay nanofiller in the HDPE matrix.

Pervaporation test by gravimetry

The pervaporation tests were based on the study carried out by Fillot *et al*. [14]. For this purpose, specimens of the nanocomposites HDPE/Clay in disc-shaped with a diameter of 4 cm and a thickness of 1 mm, were prepared by compression molding in a hydraulic press Marconi MA098 after the nanocomposites were sheared and fused in an internal mixer MH-600. The pervaporation tests were performed by using an apparatus Cup Weight Loss Method (Figure 1)

The apparatus was manufactured with stainless steel. At the bottom of the device, called a cup (Figure 1a), a known volume of fuel (gasoline) is inserted and covered with the specimens of the HDPE/Clay nanocomposites. Then, a top support (Figure 1b) is fixed to the cup by screws to press the specimens to the edges of the cup, preventing fuel leakage. The configuration of the apparatus after top support fixation is shown in Figure 1c. After adjusting the system, the device is turned from top to bottom to check for fuel leaks. Thus, fuel loss should occur only by pervaporation across nanocomposites test specimens. The test started by weighing the system (apparatus + polymer sample + fuel) and conditioning it in an oven with forced air circulation at 40ºC. The mass of the system was periodically measured as a function of the time that it remained in the oven, achieving up to 700 h. Then, the fuel mass lost was calculated, according to Equation 1.

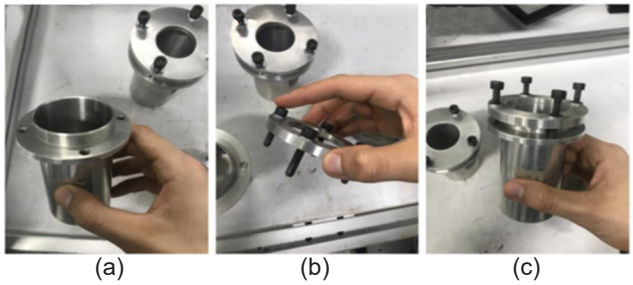

(a) (b) (c)

Figure 1. Apparatus for pervaporation test: a) Cup of fuel; b) Ring for sample fixation; c) System after ring fixation.

$$M_{fuel\ lost}\ (g) = MS_{t0}\ (g) - MS_{ti}\ (g) \quad (1)$$

where:

$M_{fuel\ lost}$ = fuel mass lost in time i

MS_{t0} = initial system mass (apparatus + polymer sample + fuel)

MS_{ti} = system mass (apparatus + polymer sample + residual fuel) in time i inside an oven at 40ºC.

Pervaporation values were calculated by using Equation 2.

$$Pi\ (g.mm/m^2) = M_{fuel\ lost}\ (g) * ST\ (mm) / SA\ (cm^2) \quad (2)$$

where:

ST = sample thickness

SA = sample area

Characterization analysis

Scanning electronic microscopy (SEM) analysis was performed on a microscopy TESCAN, model Mira 4 with electric current and tension at 300 pA and 10 keV, respectively. The cryo-fractured surfaces of the samples were gold-coated to a thickness of 15 nm prior testing, using equipment BALTEC MCS 010 under inert argon medium and an electric current at 50 mA. Micrographs were obtained with magnification from 1k to 100k.

Thermogravimetric analysis (TGA) was carried out on a NETZSCH, model STA 449 F3 with a heating rate of 10ºC.min^{-1} from 30 to 900ºC and nitrogen flow as purge and protective gas at 100 mL.min^{-1}. Samples with 12 to 15 mg were placed in alumina holders for analysis.

Mechanical tests (MT) of the nanocomposites HDPE/Clay were performed in order to verify the influence of the clay on the mechanical performance of the HDPE, i.e. whether the presence of the clay could cause negative changes to the mechanical properties of the polymer, making it unfeasible for use in the fuel tanks.

Specimens for tensile and impact tests were prepared by injection molding in an equipment DIPLOMAT model Spazio D-130W, using a temperature profile of 170, 180, 200 and 220 from feeding to nozzle and injection pressure at 100 bar.

Tensile tests were performed according to the standard ASTM D-638 in a universal machine for mechanical tests, EMIC DL3000 with a load cell of

5kN and a cross head speed of 40 mm.min 1, and Izod impact tests were conducted using an XJU-22 beam impact tester equipped with a 10.9 J pendulum, in accordance with ASTM D256.

For Dynamic-Mechanical Analysis (DMA), specimens with dimensions of 50 × 10 × 3.2 mm (length × width × thickness) were prepared from the impact samples and analyzed with an NETZSCH, model DMA 242 E Artemis in dual cantilever mode with heating rate at 2ºC.min^{-1} from -150 to 160ºC, strain frequency of 1 Hz and amplitude of 10 µm. Liquid nitrogen was used as a cooling agent.

RESULTS AND DISCUSSION

Pervaporation test

Figure 2 presents the behavior of the fuel pervaporation across specimens of HDPE and HDPE/Clay composites as a function of the time at 40ºC. For HDPE, it is noted a fast initial permeation at first hours, achieving around 2000 g.mm/m^2. Then, a constant permeation rate is verified, resulting in a fuel pervaporation around 3000 g.mm/m^2 after 700 hours at 40ºC. HDPE presents a high crystallinity degree (around 90%) which is a positive factor for barrier relating to fuel permeation [22]. On the other hand, its non-polar structure and high mobility of the polymer chain in amorphous fraction, related to a low glass transition temperature (T_g) around -120ºC, are facilitating factors for fuel permeation [23]. In HDPE/Clay composite with clay content at 1 wt.% (Clay 1%) there is a perceptible decrease in fuel permeation when compared to non-filled HDPE, arriving around 2500 g.mm/m^2 after 700 hours at 40ºC. The polar characteristic of the montmorillonite clay and impermeability of their nanoplates predictably should improve the barrier to fuel permeation of the material [24]. The lowest permeation is noted for the HDPE/Clay composite containing clay at 2 wt.% (Clay 2%), which only reaches around 500 g.mm/m^2 after 600 hours at 40ºC. The clay content at 2 wt.% should be appropriate for a uniform dispersion in the polymer matrix, causing an efficient barrier to fuel permeation and sufficient to meet the criteria established by current legislation for the evaporative emissions of hydrocarbons by fuel tanks [15,16]. The increased clay content in the composite leads to a progressive loss of the barrier to the fuel permeation. However, the permeation in HDPE/Clay composites with clay at 3 wt.% and 4 wt.% is still lower than non-filled HDPE. On the other hand, the permeation significantly increases in HDPE/Clay composite with clay content at 5 wt.% (Clay 5%), arriving 9000 g.mm/m^2 after 700 hours at 40ºC. A high clay content can make difficult the exfoliation, dispersion and distribution of the clay nanoplates into HDPE matrix. Thus, holes, voids and various structural imperfections should act as channels and pathways for fuel diffusion [25].

Scanning electronic microscopy (SEM)

Figure 3 presents SEM images of the non-filled HDPE and HDPE/Clay nanocomposites. HDPE (Figure 3a) shows a regular fracture surface without significant defects such as voids and holes. In HDPE/Clay composite containing clay at 1 wt.% (Figure 3b) the surface is similar to the non-filled HDPE. However, some inclusions of thin clay nanoplates are noted. The inclusion size, less than 13 µm, is consistent with the size of the clay, confirming its presence. For HDPE/Clay composite with clay at 2 wt.% (Figure 3c), the presence of the thin clay nanoplates as well as holes resulting from the detachment of the clay nanoplates are visible. A homogenous distribution of clay nanoplates over the surface can also be noted. These characteristics are in accordance to the highest barrier to the fuel permeation of the composite Clay 2% previously reported. For HDPE/Clay composite containing clay above 3 wt.% (Figures 3d to 3f), some differences, such as irregular concentration and larger dimensions of clay and holes, are noted. Other differences can be seen in more detail in the higher-magnification images (Figure 4). In HDPE/Clay composites containing clay at 3 and 4 wt.% (Figures 4a and 4b), the clay nanoplates are found in different orientations and a greater number of holes and voids

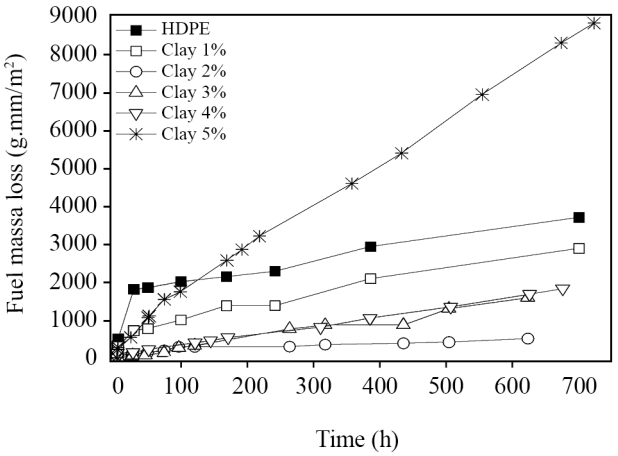

Figure 2. Apparatus for pervaporation test: a) Cup of fuel; b) Ring for sample fixation; c) System after ring fixation.

are noted, which can justify a lower barrier to fuel permeation when compared to the composite Clay 2%. The HDPE/Clay composite containing clay at 5 wt.% (Figure 4c) stands out due to the presence of large and non-exfoliated clay particles with significant voids at the filler-polymer interface. The clay content at 5 wt.% must be an excessive amount to disperse and distribute appropriated into the HDPE matrix. Thus, the shear during thermomechanical processing is insufficient for complete clay exfoliation, and the defects at the filler-matrix interface should favor increased fuel permeation across material.

Thermogravimetric analysis (TGA)

Figure 5 presents a comparison between TGA curves of the HDPE/Clay nanocomposites with different contents of clay. It is noted that there were no significant changes in the profile of the TGA curves at the temperature range corresponding to the main thermal deposition stage from 400 to 550ºC, which is related to the degradation of the HDPE polymeric structure. The residual mass observed above 500ºC is proportional to the clay content incorporated into each composite, confirming a complete thermal decomposition of the HDPE matrix at 500ºC, according to the study performed by Nunes *et al.* [26]. Depending on their chemical and physical properties, some fillers, such as zeolites, can catalyze the thermal decomposition of polyolefins. For example, zeolite ZSM-5 are effective catalysts used in cracking reactions, decreasing the required activation energy for the approach of the reagent molecules due to the action of a strong electrostatic field induced by the ionic charges of the zeolite structure [27]. On the other hand, montmorillonite clay Cloisite 30B should not affect the decomposition mechanism of the HDPE. The inert action of the clay on the thermal stability of the HDPE is a positive factor for the use of the HDPE/Clay nanocomposite in the manufacturing of fuel tanks, since the production of tanks employs thermomechanical processing such as extrusion, injection and blow molding, submitting the polymer to several conditions of shear rate and high temperatures with critical potential for polymer degradation.

Mechanical Properties

The considerable performance of mechanical properties of the HDPE is also a favorable aspect for its application in fuel tanks. Figure 6 presents the behavior of the mechanical properties by tensile tests and impact resistance for HDPE and HDPE/Clay nanocomposites as a function of the clay content. Tensile strength (Figure 6a) for non-filled HDPE is around 30 MPa. The incorporation of clay up to

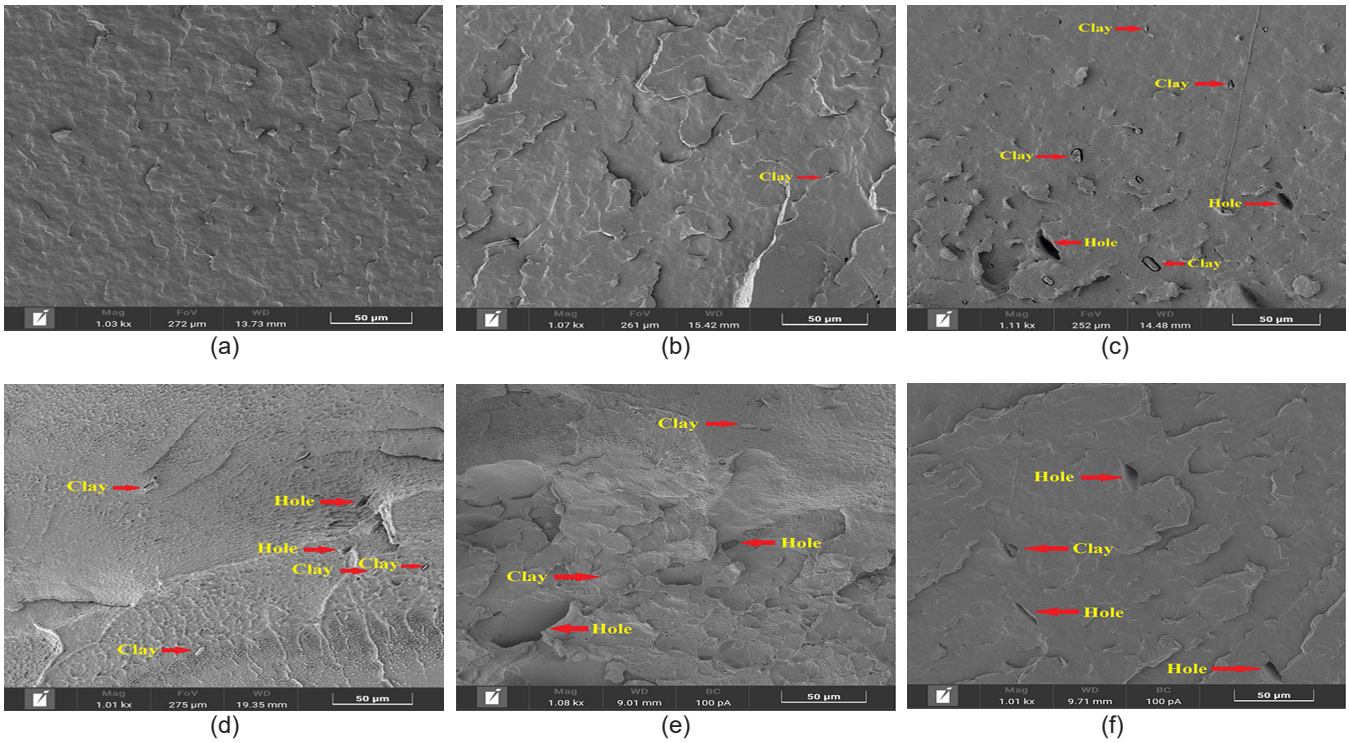

Figure 3. SEM images of the materials: a) non-filled HDPE; b) nanocomposite-clay 1wt.%; c) nanocomposite-clay 2wt.%; d) nanocomposite-clay 3wt.%; e) nanocomposite-clay 4wt.% and f) nanocomposite-clay 5wt.%.

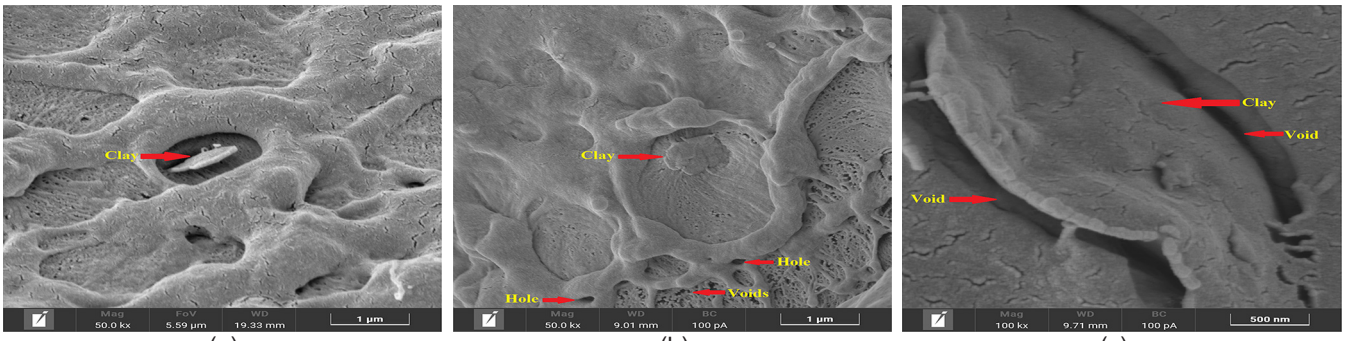

Figure 4. SEM images of the HDPE/clay composites with higher amplification: a) nanocomposite-clay 3wt.%; b) nanocomposite-clay 4wt.% and c) nanocomposite-clay 5wt.%.

4 wt.% causes a slight decrease to 29 MPa, while for nanocomposite containing clay at 5 wt.% the value arrives at 28 MPa. The filler concentration in the polymer matrix leads to particle agglomeration, causing voids and cracks in the matrix that harm the filler/matrix interface interaction and affect the mechanical properties [27-30]. On the other hand, all composites could be used for fuel tanks, considering the small changes in properties and standard deviation of the measures.

The Young modulus for the non-filled HDPE is around 350 MPa (Figure 6b). Despite some variation, there is not a significant change for the HDPE/Clay composites and all values are fluctuating within the standard deviation. This is also a positive result, which denotes an insignificant change in material performance with the incorporation of clay into the HDPE. Bartyzel *et al*. prepared HDPE/montmorillonite composites using different kinds of montmorillonite. It was noted only slight changes in the Young modulus of the nanocomposites when compared to the unfilled HDPE [31].

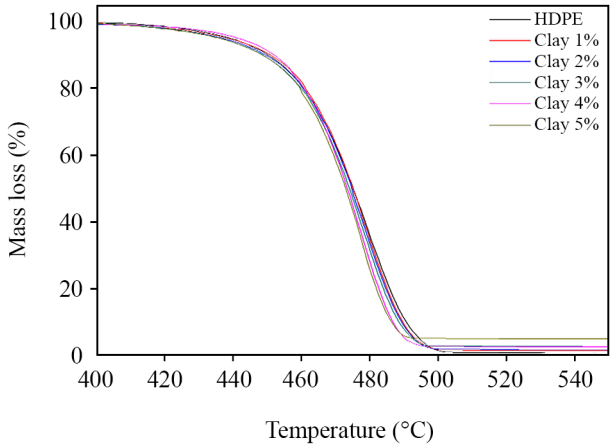

Figure 5. Mechanical properties of the materials: a) tensile strength; b) Young modulus; c) Elongation-at -break and d) impact resistance.

For elongation-at-break (Figure 6c), the HDPE presents values around 32%. A slight and progressive decrease is verified for HDPE/Clay composites as a function of clay content, arriving up to 26% for clay content at 5 wt.%. This behavior is expected since the filler presents lower strain than the polymer matrix. It can also be stated that the composites became more rigid and brittle with the increase in filler content [31,32]. However, the elongation-at-break for composites remains significant and sufficient to meet the requirements for application in fuel tanks. Al-Jumaili *et al*. also verified a progressive decrease in elongation-at-break in polyethylene/montmorillonite composite as a function of increased montmorillonite content. This effect could be due to a restriction in slipping movement of chains during deformation caused by the presence of filler [33].

Similar to the Young modulus, the impact resistance shows insignificant changes with values ranging around 36 to 38 kJ/m^2 and within the standard deviation error. Only the HDPE/Clay composites containing clay at 5 wt.% presents a more significant decrease in impact resistance at 30 kJ/m^2. Jiang *et al*. have also noted insignificant change in impact resistance of HDPE containing reinforcement at low concentration. With higher filler content, there are filler agglomerations that act as points of tension concentration as well as the polymer matrix bearing all the loads and plastic deformation occurs which consumes energy until resin fracture [34].

In general, the tensile and impact mechanical properties of the HDPE, mainly with low clay content, are not significantly affected by the incorporation of montmorillonite clay. Thus, the barrier to fuel permeation in the HDPE/Clay composites with up to 4 wt.% of clay shows even greater potential for application since required mechanical properties remain at appropriate levels.

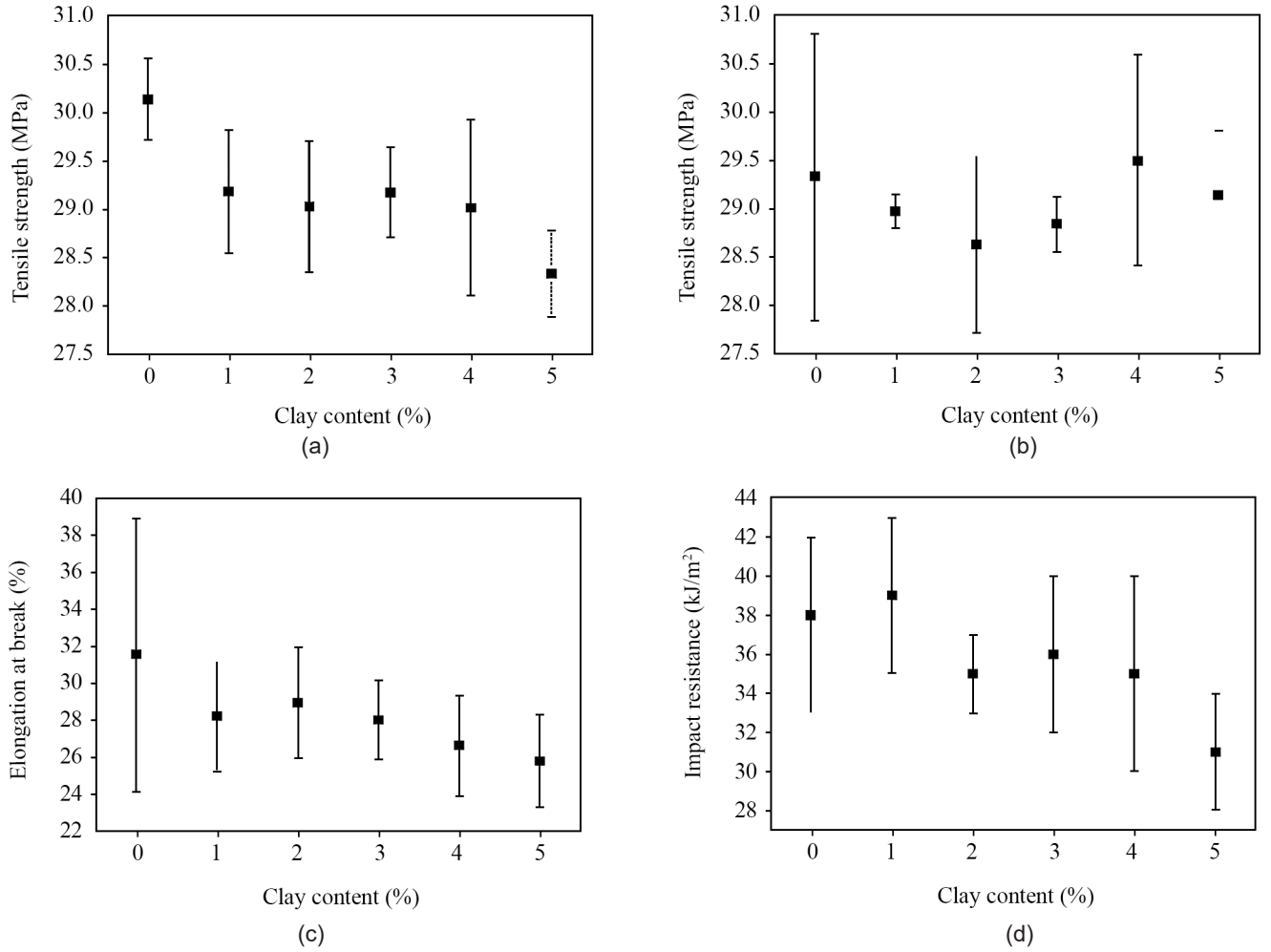

Figure 6. Mechanical properties of the materials: a) tensile strength; b) Young modulus; c) Elongation-at-break and d) impact resistance.

Dynamical-Mechanical Analysis (DMA)

DMA is an important analysis to identify polymer relaxations [35]. Thus, changes related to the polymer/filler interactions can be verified. Figure 7 presents the DMA results of the materials. In Figure 7a, lower values of the storage modulus are observed for DMA curve of the unfilled HDPE when compared to the HDPE/Clay nanocomposites. On the other hand, there are no significant changes in curve profiles of the materials. The incorporation of mineral fillers into the polymers predictably leads to an increased hardness and elastic modulus due to the restrictions on molecular mobility caused by the fillers [36]. Savini and Oréfice also noted an increase in storage modulus of the HDPE when filler was incorporated into the material, which attributes the restriction of the molecular mobility of this semicrystalline polymer to a physical barrier caused by the filler particles [36]. DMA is an accurate technical for analyzing viscoelastic behavior in polymer systems, and its results showed a higher storage modulus in HDPE/Clay nanocomposites when compared to the non-filled HDPE. Despite Young modulus (Figure 6b) pointing to a similar trend, the lower precision of the measures of the mechanical test made unfeasible an accurate definition of the behavior.

The storage modulus curves also show two noticeable relaxations, corresponding the glass transition (T_g) below -100ºC and the melting point around 125ºC when the signal is collapsed.

Figure 6b shows a comparison between loss factor curves (tanδ) of the materials. Herein, the T_g signal is evident at temperatures next to -120ºC for HDPE. In general, the T_g signals for HDPE/Clay composites are narrower. However, there is no significant shift in values related to the T_g temperature between the materials that could indicate changes in mobility and relaxation of polymer chains.

According DMA results, as well as the other characterization analyses, the clay incorporation

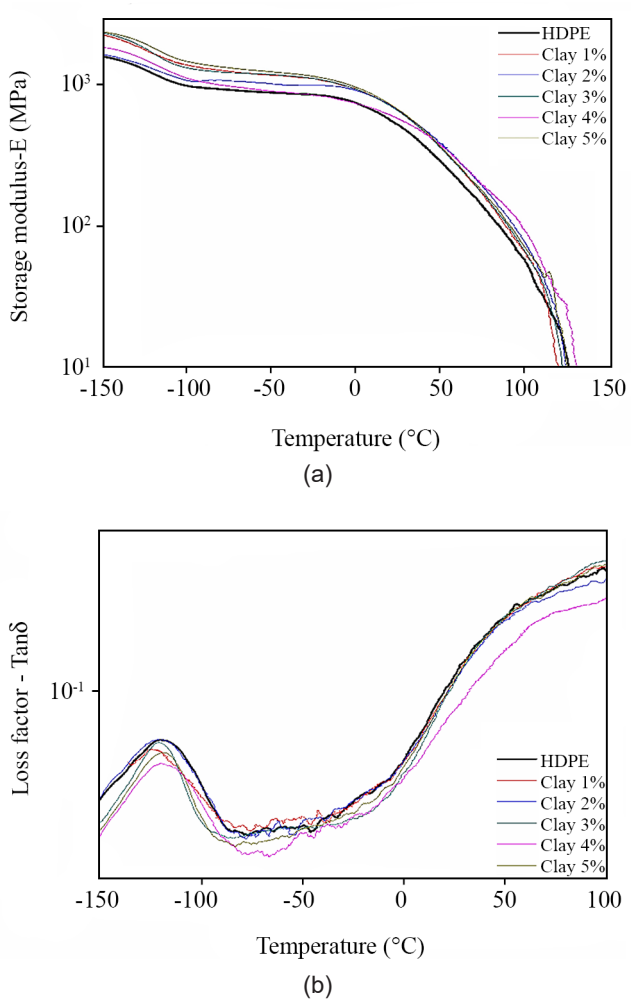

Figure 7. DMA curves of the materials: a) Storage modulus – E'; b) Loss factor - Tanδ.

does not significantly modify important thermal and mechanical properties of the polymer, while the barrier for fuel permeation is greatly improved.

CONCLUSION

The incorporation of the organically modified montmorillonite clay Cloisite 30B up to 4wt.% into high-density polyethylene caused significant improvement of the barrier to the fuel permeation of the polymer, and the clay content at 2wt.% has produced the best result. On the other hand, the incorporation of the filler at 5wt.% decreased the barrier to fuel permeation when compared to the non-filled HDPE. The appropriate dispersion and distribution of the filler at low content in polymer matrix, together with their hydrophilic and impermeability properties, should be the main causes in barrier improvement. There were no significant changes in thermal stability of the polymer with the clay incorporation, which is a positive factor considering the thermomechanical processing conditions where the material is submitted to the manufacturing process of the fuel tanks. Despite the incorporation of the clay increases the polymer hardness, other mechanical properties are not significantly affected, remaining an appropriated mechanical performance of the material for manufacturing of fuel tanks. The level of barrier to the fuel permeation for HDPE/clay composites containing clay at 2 wt.% meets the requirements of the standards PL7 and PL8. Thus, this material can be used for the manufacture of the fuel tanks, substituting the use of conventional materials (copolymers) and methods (fluoridation). This should represent substantial savings in production costs that simplify the process overall. Other economic and environmental benefits can also be achieved using the HPDE/Clay nanocomposites, since post-industrial waste generated from defective fuel tanks can be mechanically recycled on the same productive cycle. The recycling of the post-consumer waste from fuel tanks should also be made possible.

ACKNOWLEDGEMENTS

The authors would like to thank the IPA Automotive Products Industry RGS Ltda - Brazil for supplying the materials as well as the Fundação de Amparo à Pesquisa do Estado de São Paulo - FAPESP (Proc. 2020/14318-6 and 2024/17297-0) and Conselho Nacional de Desenvolvimento Científico e Tecnológico - CNPq (Proc. 305288/2023-7) for their financial support.

AUTHORS' CONTRIBUTIONS

Guilherme Gama Simão: investigation, characterization and writing.

Clodoaldo Saron: project administration, investigation, writing, editing and review.

CONFLICT OF INTEREST

The authors declare no conflict of interest.

REFERENCES

1. Li J, Ge Y, Wang X, Zhang M, Wang H (2024)

Comparison of tailpipe carbonyls and volatile organic compounds emissions from in-use gasoline/CNG bi-fuel vehicles. J Environ Sci 135: 619-629
2. Kęska A (2023) The actual toxicity of engine exhaust gases emitted from vehicles: The development and perspectives of biological and chemical measurement methods. ACS Omega 8: 24718-24726
3. Gis W, Gis M, Pielecha J, Skobiej K (2021) Alternative exhaust emission factors from vehicles in on-road driving tests. Energies 14: 3487
4. Yang HH, Dhital NB, Cheruiyot NK, Wang LC, Wang SZ (2021) Effects of road grade on real-world tailpipe emissions of regulated gaseous pollutants and volatile organic compounds for a Euro 5 motorcycle. Atmos Pollut Res 12: 101167
5. Dlamini NG, Fujimura K, Yamasue E, Okumura H, Ishihara KN (2011) The environmental LCA of steel vs HDPE car fuel tanks with varied pollution control. Int J Life Cycle Assess 16: 410-419
6. Berger K, Keimel C, Helfer E, Haar B, Mattausch H, Riess G, Kern W (2017) The effects of e-beam crosslinking of LDPE on the permeation of hydrocarbons. J Appl Polym Sci 134: 44968
7. Wang W, Zhang J, Ge X, Shi Y, Tang X, Zhang Z, Chen W, Qian G, Cao Y, Ye G, Xia C, Feng X, Li L, Duan X, Zhou X, Guo X, Van Geem KMV, Zhang J (2025) Toward carbon neutrality: Single-step polyethylene upcycling to BTX using Ni-ZSM-5 catalyst. AIChE J 71: E18890
8. Mun SC, Kim MJ, Cobos M, Gu L, Macosko CW (2019) Strategies for interfacial localization of graphene/polyethylene-based cocontinuous blends for electrical percolation. AIChE J 65: e16579
9. Lee JH, Kim YW, Jung JK (2023) Investigation of the gas permeation properties using the volumetric analysis technique for polyethylene materials enriched with pure gases under high pressure: H_2, He, N_2, O_2 and Ar. Polymers 15: 4019
10. Klopffer MH, Flaconneche B, Odru P (2007) Transport properties of gas mixtures through polyethylene. Plast Rubber Compos 36: 184-189
11. Ravi SS, Osipov S, Turner JWG (2023) Impact of modern vehicular technologies and emission regulations on improving global air quality. Atmosphere 14: 1164
12. Monti M, Perin E, Conterosito E, Romagnolli U, Muscato B, Girotto M, Scrivani MT, Gianotti V (2023) Development of an advanced extrusion process for the reduction of volatile and semi-volatile organic compounds of recycled HDPE from fuel tanks. Resour Conserv Recycl 188: 106691
13. Ferrarese C, Franzetti J, Selleri T, Suarez-Bertoa R (2024) VOC emissions from Euro 6 vehicles. Environ Sci Eur 36: 27
14. Fillot LA, Ghiringhelli S, Prebet C, Rossi S (2015) Biofuels barrier properties of polyamide 6 and high density polyethylene. Oil Gas Sci Technol 70: 335-351
15. Brazil. Programa de controle de emissões veiculares (Proconve – L7). https://www.gov.br/ibama/pt-br/assuntos/emissoes-e-residuos/emissoes/programa-de-controle-de-emissoes-veiculares-proconve
16. Brazil. Programa de controle de emissões veiculares (Proconve–L8). https://conama.mma.gov.br/index.php?option=com_sisconama&task=documento.download&id=22296
17. Yeh JT, Chen CH, Shyu WD (2001) Gasoline permeation resistance of the as-blow-molded and annealed polyethylene, polyethylene/polyamide, and polyethylene/modified polyamide bottles. J Appl Polym Sci 81: 2827-2837
18. Warr LN, Thombare BR, Sudheer Kumar R, Peltz M, Podlech C, Grathoff GH (2024) Determining the stoichiometric composition of Wyoming montmorillonite using improved transmission electron microscopy-energy dispersive X-ray (TEM-EDX) techniques. Clays Clay Miner 72: e25
19. El-Sheikhy R, Al-Shamrani M (2017) Interfacial bond assessment of clay-polyolefin nanocomposites CPNC on view of mechanical and fracture properties. Adv Powder Technol 28: 983-992
20. Jain MR, Jain C, Shah S, Jain RC (2014) Preparation and characterization of HDPE/Silane-modified nanoclay composites for application in fuel storage. SAE Int J Mater Manuf 07: 225-232
21. Ma Y, Yang J, Wang X, Tian M, Yang W, Xie P (2023) Preparation of high-density polyethylene/montmorillonite nanocomposites with high gas barrier by micro-nano torsional laminated

extrusion. Polym Compos 44: 6747-6757
22. Sabet M, Soleimani H (2019) Broad studies of graphene and low-density polyethylene composites. J Elastomers Plast 51: 527-561
23. Hadi AJ, Hadi GJ, Yusoh KB, Najmuldeen GF, Hasany SF (2017) Prediction of experimental measurement data for high density polyethylene and polypropylene solubility in organic solvents. Chem Prod Process Model 12: 78
24. Yousefi V, Mohebbi-Kalhori D, Samimi A (2018) Application of layer-by-layer assembled chitosan/montmorillonite nanocomposite as oxygen barrier film over the ceramic separator of the microbial fuel cell. Electrochim Acta 283: 234-247
25. Singh M, Mehta R, Verma SK, Biswas I (2018) Effect of addition of different nano-clays on the fumed silica-polyethylene glycol based shear-thickening fluids. Mater Res Exp 5: 014001
26. Nunes MBS, Farias AFF, Medeiros ES, Oliveira JE, Santos IMG, Carvalho LH, Santos ASF (2021) The effect of clay organophilization on wood plastic composite (WPC) based on recycled high density polyethylene (HDPE) and coir fiber. Prog Rubber Plast Recycl Technol 37: 394-411
27. El-Shekeil YA, Sapuan SM, Abdan K, Zainudin ES (2012) Influence of fiber content on the mechanical and thermal properties of Kenaf fiber reinforced thermoplastic polyurethane composites. Mater Des 40: 299-303
28. da Silva EF, dos Santos Luiz D, de Andrade Junior AJ, Saron C (2025) Catalytic action of natural clay on polyolefins during reactive processing. Iran Polym J 34: 1721-1729
29. Moreno DDP, Saron C (2017) Low-density polyethylene waste/recycled wood composites. Compos Struct 176: 1152-1157
30. Chollakup R, Tantatherdtam R, Ujjin S, Sriroth K (2011) Pineapple leaf fiber reinforced thermoplastic composites: Effects of fiber length and fiber content on their characteristics. J Appl Polym Sci 119: 1952-1960
31. Bartyzel O, Majka TM, Leszczy A, Pielichowski K. (2013) Mechanical properties of HDPE/ recycled montmorillonite composites. In: Modern Polymeric Materials for Environmental Applications, 5th International Seminar including COST MP1105 Workshop (pp.11-16), 1st ed, Wydawnictwo Naukowo-Techniczne, Eds: Krzysztof Pielichowski
32. Wang YZ, Zou CY, Bai N, Su QF, Song LX, Li XL (2023) Effect of octene block copolymer (OBC) and high-density polyethylene (HDPE) on crystalline morphology, structure and mechanical properties of octene random copolymer. Polymers 15: 3655
33. Al-Jumaili SK, Alkaron WA, Atshan MY (2023) Mechanical, thermal, and morphological properties of low-density polyethylene nanocomposites reinforced with montmorillonite: Fabrication and characterizations. Cogent Eng 10: 2204550
34. Allahverdi A, Ehsani M, Janpour H, Ahmadi S (2012) The effect of nanosilica on mechanical, thermal and morphological properties of epoxy coating. Prog Org Coat 75: 543-548
35. Jiang L, Wang X, Zhou Y (2024) Effects of fiber characteristics on tensile and impact properties of long fiber reinforced high-density polyethylene. Polym Compos 45: 11138-11148
36. Savini G, Oréfice RL (2020) Comparative study of HDPE composites reinforced with microtalc and nanotalcs: high performance filler for improving ductility at low concentration levels. J Mater Res Technol 9: 16387-16398